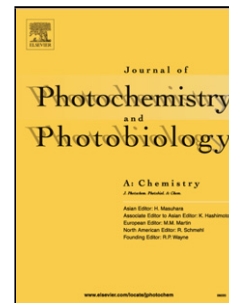


Journal Pre-proof

Fluorescence quenching of triarylamine functionalized phenanthroline-based probe for detection of picric acid

P.A. Parvathy, R. Dheepika, R. Abhijnakrishna, P.K.M. Imran, S. Nagarajan



PII: S1010-6030(20)30579-7

DOI: <https://doi.org/10.1016/j.jphotochem.2020.112780>

Reference: JPC 112780

To appear in: *Journal of Photochemistry & Photobiology, A: Chemistry*

Received Date: 6 May 2020

Revised Date: 26 June 2020

Accepted Date: 13 July 2020

Please cite this article as: Parvathy PA, Dheepika R, Abhijnakrishna R, Imran PKM, Nagarajan S, Fluorescence quenching of triarylamine functionalized phenanthroline-based probe for detection of picric acid, *Journal of Photochemistry and Photobiology, A: Chemistry* (2020), doi: <https://doi.org/10.1016/j.jphotochem.2020.112780>

This is a PDF file of an article that has undergone enhancements after acceptance, such as the addition of a cover page and metadata, and formatting for readability, but it is not yet the definitive version of record. This version will undergo additional copyediting, typesetting and review before it is published in its final form, but we are providing this version to give early visibility of the article. Please note that, during the production process, errors may be discovered which could affect the content, and all legal disclaimers that apply to the journal pertain.

© 2020 Published by Elsevier.

Fluorescence quenching of triarylamine functionalized phenanthroline-based probe for detection of picric acid

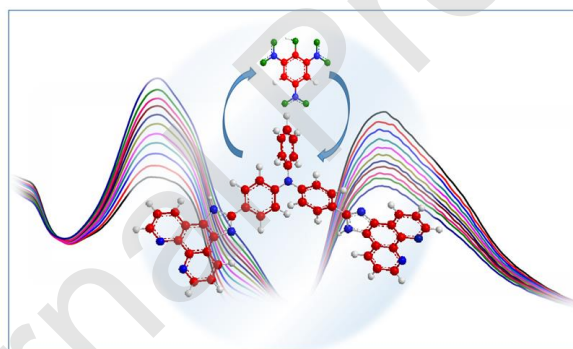
P. A. Parvathy,^a R. Dheepika,^a R. Abhijnakrishna,^a P.K.M. Imran,^b S. Nagarajan^{a*}

^aDepartment of Chemistry, Central University of Tamil Nadu, Thiruvavur-610 005, India.

^b Department of Chemistry, Islamiah College, Vaniyambadi- 635 752, India.

*snagarajan@cutn.ac.in

Graphical Abstract



Highlights

- Designed and synthesized new triarylamine based phenanthroline.
- Molecules act as good sensor for nitro aromatics.

- Picric acid enhanced the absorption and quenched the fluorescence maxima.
- Selective detection of picric acid at micro mole concentration.
- FRET mechanism is observed.

Abstract

Detection of toxic nitro aromatic compounds (NAC) using a cost-effective fluorescence sensing method have gained global attention. The current work demonstrates the selective sensing of picric acid using imidazo[4,5-*f*]-1,10-phenanthroline-triarylamine. The specific interaction mode of sensor molecules with NACs is established by absorption and emission spectroscopic methods. Remarkably, a new band appeared in the range of 420 to 480 nm. This new band increased the probability of overlap of the absorption with the emission spectra and ensures the FRET mechanism. The presence of electron rich methoxy group on TAA side arm improved the interaction with electron deficient picric acid with a binding constant of $1.46 \times 10^5 \text{ M}^{-1}$. The linearity of the Stern-Volmer plot confirms the mechanism is static quenching. The detection limit was calculated to be at micro molar level for all the four compounds. Density functional theory was employed to study the HOMO - LUMO of the compounds and informs that the energy transfer is more feasible from electron rich sensor molecule to picric acid. These molecules can act as efficient fluorescence sensor for selective picric acid detection.

Keywords: Quenching; sensing; fluorescence; phenanthroline; triarylamine; picric acid.

1. Introduction

Sensing of nitro aromatic compounds (NAC) is one of the imperative research topics due to their toxicity and explosive nature [1]. Among many NACs, picric acid (PA,

2,4,6-trinitrophenol) gained special attention due to its adverse health issues such as allergy, diarrhoea, and neurological disorders [2]. PA has wide spectrum of applications in pharmaceutical and dye industries [3]. In addition, high solubility of PA makes the situation more perilous; leads to ground water and soil pollution. Considering the wide array of applications and effects, picric acid sensing has been a mainstream research in the past decades. Various practices such as chromatography [4], membrane electrode technique [5], and spectrophotometric techniques [6] have been investigated for sensitive and selective detection of picric acid. However, apart from spectrophotometry, other techniques have the drawbacks of real-time sample analysis, costly, and difficulty in handling. As a result of continuous efforts, fluorescent chemo-sensors have been recognized as an easy, robust alternative method and applied in many fields like biology, pharmacology, and environmental sciences [7]. Design of the molecule is the first important strategy to achieve a good sensor. NACs are electron deficient in nature [8] and hence designing electron-rich molecules facilitates sensing of picric acid via better interaction.

Different types of sensor molecules are inspected for detection of PA and distinct mechanisms are proposed [9, 10]. Recently, Sushil Kumar and co-workers [11] reported palladium-based metal organic frame work as sensor for picric acid. With one Pd unit, the interaction was through hydrogen bonding and π -electron interaction, while with two Pd units, picric acid perfectly fits in the cavity of the macrocycle. Laxmi *et al.* [12] reported aggregation induced emission probes for the receptor free detection of picric acid using a copolymer poly(2,7-(9,9- dioctylfluorene)-co-3,4-diphenyl-2,5-distyrylthiophene) and explained the mechanism through fluorescence resonance transfer and photoinduced energy transfer processes [13-15]. Gel based sensor molecules are reported by Bhalla *et al.* [16] in which pentacene quinone derivative formed supramolecular aggregates to detect PA in ppb level.

Triarylamines (TAA) are promising candidates for many applications including organic electronics and sensing [17-20, 22]. They are capable of undergoing two photon absorption and suitable for biological applications [19, 21]. Structural modification of the non-planar structure resulted in aggregation induced emission and utilized in toxic metal ions [23, 24] nitro compounds [25-30] sensing. Palas *et al.*,

reported a triphenylamine based fluorophore for detection of PA with intramolecular photoinduced electron transfer mechanism between electron rich triphenylamine and electron deficient nitroaromatics with detection limit of 449 ppb [31]. Aniketchowdary *et al.*, stated that the PA undergone deprotonation and resonance energy transfer with the analyte in solution state. In solid state, exciton migration was observed after analyte binding: as a result, fluorescence quenching was amplified [32].

In this investigation, we have designed and synthesised new TAA molecules via focussed microwave assisted synthesis with high purity and yield. The interaction between the synthesized molecules and the NACs is investigated by absorption and emission spectroscopic techniques. Density functional theory (DFT) is also employed to scrutinize the structure and frontier molecular orbitals of the molecules and the targets to get insight about their interaction. The core objective of this investigation is to develop fluorescence as an easy and robust technique for NAC sensing.

2. Experimental

2.1 Materials and methods

All the starting materials are purchased from commercial sources and used as received. Microwave assisted synthesis was performed using CEM microwave synthesizer. All the reactions and chromatographic separations were monitored by pre-coated thin layer chromatographic plates. Column chromatography was carried out with slurry packed activated silica gel (100-200 mesh). UV-Vis absorption spectra were recorded using Jasco V-670 spectrophotometer. Emission spectra were obtained using Perkin Elmer LS 55 spectrofluorimeter. FT-IR spectra were recorded using Perkin Elmer spectrometer. Electron spray ionization (ESI) high resolution mass spectra were recorded in Thermo scientific Exactiveplus UHPLC mass spectrometer. The molecules were optimized at the 6-31G basis level of DFT using Gaussian. The frontier molecular orbital values (HOMO and LUMO) were extracted using GaussView software.

2.2 Synthesis of compounds

The precursor molecule **1** was synthesized by Vilsmeier Haack reaction of triphenylamine. It was further subjected to iodination in presence of potassium iodide and iodate to yield compound **2** (**Scheme 1**). The compounds were purified by column chromatography. Phenanthroline was oxidized in vigorous condition (NaBr, H₂SO₄, HNO₃, 100 °C) to yield phenanthroline dione, **6**. The detailed synthetic procedures are given in the supporting information.

2.3 General procedure for Suzuki coupling, 3-5

Compound **2** (1 eq) was dissolved in THF and Pd(PPh₃)₄ (0.08 eq) was added under nitrogen atmosphere. 2 M aqueous Na₂CO₃ was added and stirred for 20 min at room temperature. Boronic acid (1.1 eq) was added and refluxed for 7 h. Completion of the reaction was monitored by TLC. Reaction mixture was cooled to room temperature filtered over celite to remove Pd. Then it was extracted with DCM/water and dried over Na₂SO₄. Solvent was removed under reduced pressure. Purification was done by liquid column chromatography (Stationary phase: Silica gel (100-200 mesh), eluent: EtOH/Hexane).

4,4'-((4-Phenyl)phenylamino)dibenzaldehyde, 3: Yield: 83%. Yellow solid. ¹H NMR (400 MHz, CDCl₃, δ in ppm): 9.91 (s, 2H); 7.802 (m, 4H); 7.662 (m, 4H); 7.426 (m, 3H); 7.214 (m, 6H). ¹³C NMR (100 MHz, CDCl₃, δ in ppm): 151.95, 144.68, 139.21, 131.43, 131.37, 128.93, 128.71, 127.10, 126.93, 123.10, 123.02, 122.96.

4,4'-((4'-Methoxy(4-phenyl))phenylamino)dibenzaldehyde, 4: Yield: 66%. Yellow solid. ¹H NMR (400 MHz, CDCl₃, δ in ppm): 9.906 (s, 2H); 7.795 (d, J=8.4Hz, 3H); 7.553 (m, 4H); 7.232 (m, 7H); 6.998 (d, J=7.2Hz, 2H); 3.866 (s, 3H). ¹³C NMR (100 MHz, CDCl₃, δ in ppm): 190.62, 159.40, 151.97, 144.05, 138.74, 132.45, 131.35, 128.22, 127.98, 127.21, 122.84, 114.37, 55.38.

4,4'-((4-(Thiophen-3-yl))phenylamino)dibenzaldehyde 5: Yield: 63%. Yellow solid. ¹H NMR (400 MHz, CDCl₃, δ in ppm): 9.907 (s, 2H); 7.795 (d, J=8Hz, 4H);

7.617 (d, $J=7.6\text{Hz}$, 2H); 7.434 (m, 3H); 7.224 (m, 6H): ^{13}C NMR (100 MHz, CDCl_3 , δ in ppm): 190.61, 151.88, 144.35, 141.16, 133.79, 131.41, 128.10, 127.20, 126.64, 126.09, 122.89, 120.59

2.4 General procedure for microwave assisted synthesis of imidazo[4,5-f]-1,10-phenanthroline

A mixture 1,10-phenanthroline-5,6- dione (**3**) (2.5 eq), TPA dialdehyde (**1**) or Suzuki coupled compound (**4-6**) (1 eq), ammonium acetate (30 eq), and glacial acetic acid was heated at 100 °C for 20 min under microwave conditions (power: 150, pressure: 270, pre-stirring time: 1min). Completion of the reaction was monitored by TLC and after completion the reaction mixture was poured to ice-cold water. The solid was filtered and washed with hot water three times and with ammonia solution. The product was dried under vacuum.

N,N-Bis(4-1H-imidazo[4,5-f]-1,10-phenanthrolin-2-yl)-[1,1'-biphenyl]-4-amine, 7: Yield: 80%. Reddish orange solid. m.p: 562 °C. ^1H NMR (400 MHz, CDCl_3 , δ in ppm): 13.639 (s, 2H); 9.04 (s, 4H); 8.929 (d, $J=7.6\text{ Hz}$, 4H); 8.255 (d, $J=7.6\text{ Hz}$, 4H); 7.842 (s, 4H); 7.461 (m, 2H); 7.311 (d, $J=7.6\text{ Hz}$, 4H); 7.251 (d, $J=6.8\text{ Hz}$, 3H): ^{13}C NMR (100 MHz, CDCl_3 , δ in ppm): 150.92, 148.39, 148.19, 146.75, 144.05, 143.84, 136.25, 130.44, 130.04, 128.11, 126.74, 125.86, 125.05, 124.91, 124.14, 123.84, 123.58. MS (ESI) m/z calcd for $\text{C}_{44}\text{H}_{27}\text{N}_9$ $[\text{M}+\text{H}]^+$ 682.2389; found, 682.2451.

N,N-Bis(4-(1H-imidazo[4,5-f]-1,10-phenanthrolin-2-yl)phenyl)-[1,1'-biphenyl]-4-amine, 8: Yield: 95%. Orange solid. ^1H NMR (400 MHz, CDCl_3 , δ in ppm): 9.237 (m, 4H); 8.914 (m, 4H); 8.269 (m, 4H); 7.937 (m, 4H); 7.745 (m, 4H); 7.481 (m, 2H); 7.338 (m, 6H); 7.029 (m, 1H): ^{13}C NMR (100 MHz, CDCl_3 , δ in ppm): 151.01, 148.23, 147.97, 147.91, 136.30, 130.09, 130.05, 129.47, 128.50, 128.27, 127.75, 126.81, 126.70, 125.70, 125.36, 125.10, 124.38, 124.36, 124.22, 123.67, 123.61. MS (ESI) m/z calcd for $\text{C}_{50}\text{H}_{31}\text{N}_9$ $[\text{M}-\text{H}]^-$ 757.2602; found, 756.2633.

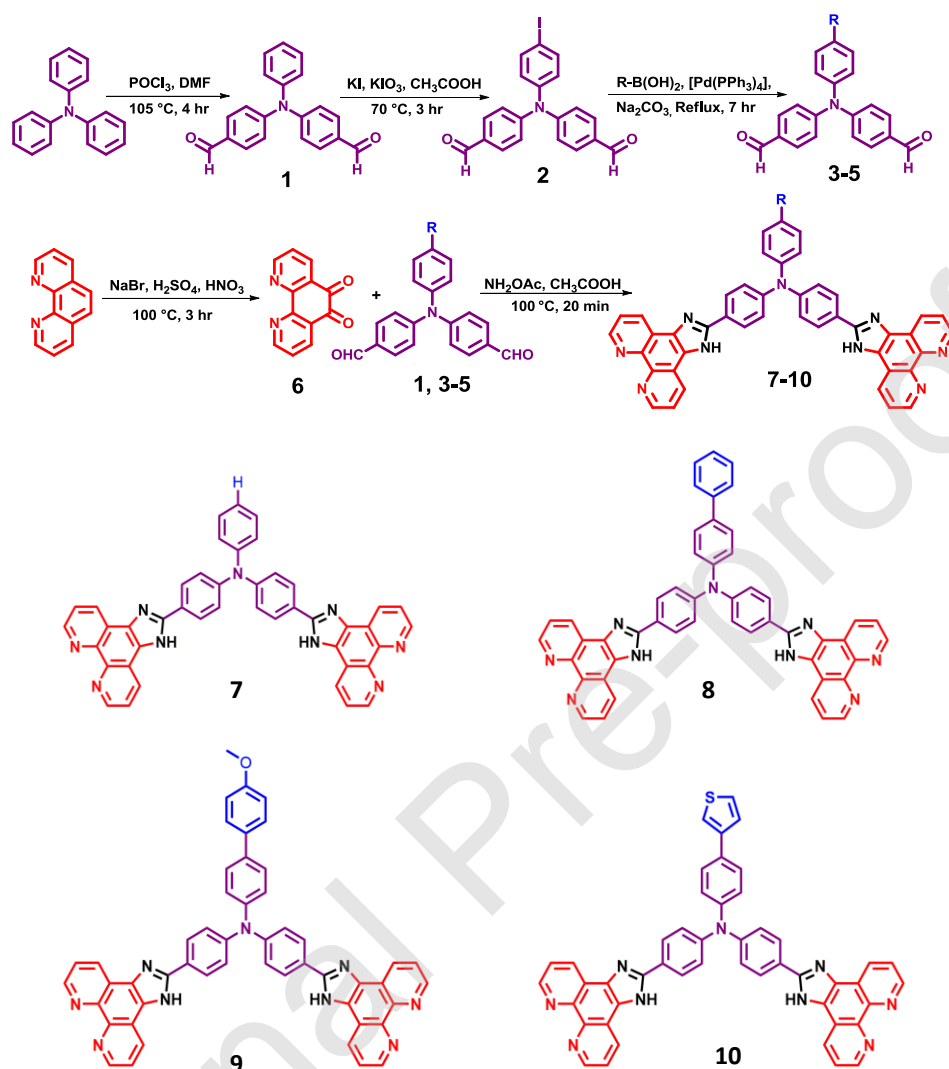
N,N-Bis(4-(1H-imidazo[4,5-f]-1,10-phenanthrolin-2-yl)phenyl)-4'-methoxy-[1,1'-biphenyl]-4-amine, 9: Yield: 93%. Orange solid. ^1H NMR (400 MHz, CDCl_3 , δ in

ppm): 13.713 (s, 2H); 9.045 (s, 4H); 8.927 (d, J=6.8 Hz, 4H); 8.271 (d, J=7.2 Hz, 4H); 7.764 (m, 4H); 7.657 (m, 4H); 7.36 (m, 4H); 7.282 (m, 2H); 7.042 (m, 3H); 3.81 (m, 3H); ^{13}C NMR (100 MHz, CDCl_3 , δ in ppm): 159.32, 150.84, 148.36, 145.54, 144.07, 143.90, 136.37, 136.12, 132.19, 130.05, 128.13, 127.98, 126.74, 126.68, 126.02, 125.08, 124.17, 124.01, 123.55, 119.78, 114.84, 55.35. MS (ESI) m/z calcd for $\text{C}_{51}\text{H}_{33}\text{N}_9\text{O}[\text{M}-\text{H}]^-$ 786.2808; found, 786.2739.

N,N-Bis(4-(1H-imidazo[4,5-f]-1,10-phenanthrolin-2-yl)phenyl)-4-(thiophen-3-yl)aniline, 10: Yield: 90%, Orange solid. ^1H NMR (400 MHz, CDCl_3 , δ in ppm): 13.699 (s, 2H); 9.042 (s, 4H); 8.926 (d, J=8Hz, 4H); 8.268 (d, J=8Hz, 4H); 7.805 (m, 7H); 7.671 (s, 1H); 7.594 (d, J=2.4Hz, 1H); 7.355 (d, J=8Hz, 4H); 7.262 (d, J=7.2Hz, 2H); ^{13}C NMR (100 MHz, CDCl_3 , δ in ppm): 151.15, 151.04, 150.89, 148.28, 148.19, 148.09, 145.61, 143.96, 143.80, 141.49, 141.32, 131.69, 130.11, 128.37, 128.12, 127.99, 127.62, 126.50, 125.86, 125.05, 124.2, 123.99, 123.99, 123.79, 123.71, 121.02. MS (ESI) m/z calcd for $\text{C}_{48}\text{H}_{29}\text{N}_9\text{S}[\text{M}+\text{H}]^+$ 764.2266; found, 764.2327.

3. Results and discussions

The sensing molecules are designed with highly conjugated triarylamine - phenanthroline systems connected via an azole ring. TAA part is further functionalized with electron rich thiophene and methoxyphenyl groups to improve the interaction with electron deficient NACs. In addition, the imidazole nitrogen can also facilitate the interaction through H-bonding. The target molecules **7-10** are obtained by microwave assisted synthesis (Scheme 1) and characterized using spectroscopic techniques. Condensation of phenanthroline, **3** with TAA aldehyde in the presence of acetic acid and ammonium acetate at 100 °C was carried out in CEM microwave synthesizer and the products were obtained in high purity and good yield. IR spectra are given in Figures S1 to S4 (supporting information). The peaks in the range of 1590-1600 cm⁻¹ and 1445-1475 cm⁻¹ corresponds to C=N and C=C stretching, respectively. ESI-Mass spectrometry analysis confirmed formation of final compounds **7-10** (Figure S5-S8 in supporting information).



Scheme 1. Synthetic route and molecular structure of functionalized imidazo[4,5-*f*]-1,10-phenanthrolines

The NMR spectra are given in the **Figures S9-S22** in supporting information. For compound **5**, the methoxy carbon resonates at 55 ppm. The spectra of the compounds

shows characteristic peak for N-H in highly de-shielded region and aromatic protons are resonating at 7-9.2 ppm. For the molecule **9**, the methoxy protons resonated at 3.8 ppm. The molecular structure of target compounds is shown in **Scheme 1**.

3.1 Optical properties

To evaluate the photophysical properties of new compounds **7-10**, their absorption and emission spectra are recorded in DMSO at 10^{-5} M concentration. Spectra are given in the **Figure 1** and the data are represented in **Table 1**. Absorption spectra exhibited two prominent peaks around 380 and 285 nm attributed to $n-\pi^*$ and $\pi-\pi^*$ transitions, respectively.

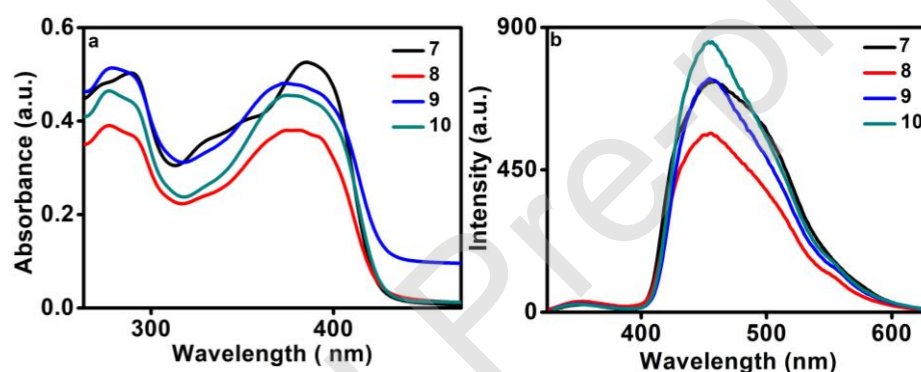


Figure1. (a) Absorption and (b) emission spectra of **7-10**

Table 1. Photophysical properties of compounds **7-10**

C. No	λ_{Abs} (nm)	λ_{Em} (nm)	Stokes' shift (nm)	ϵ (1×10^{-4}) $M^{-1} cm^{-1}$
7	385	459.5	74.5	5.2
8	381	455.5	74.5	3.8
9	373	454.0	81	4.8
10	375	453.5	78.5	4.5

Emission spectra shows single emission peak in the region of 450-460 nm. Among the four new compounds, compound **10** has higher emission intensity due to the presence of electron donating thiophene group [33]. Polar medium creates charge separation in the excited state of the molecule and thereby changes the geometry [34, 35].

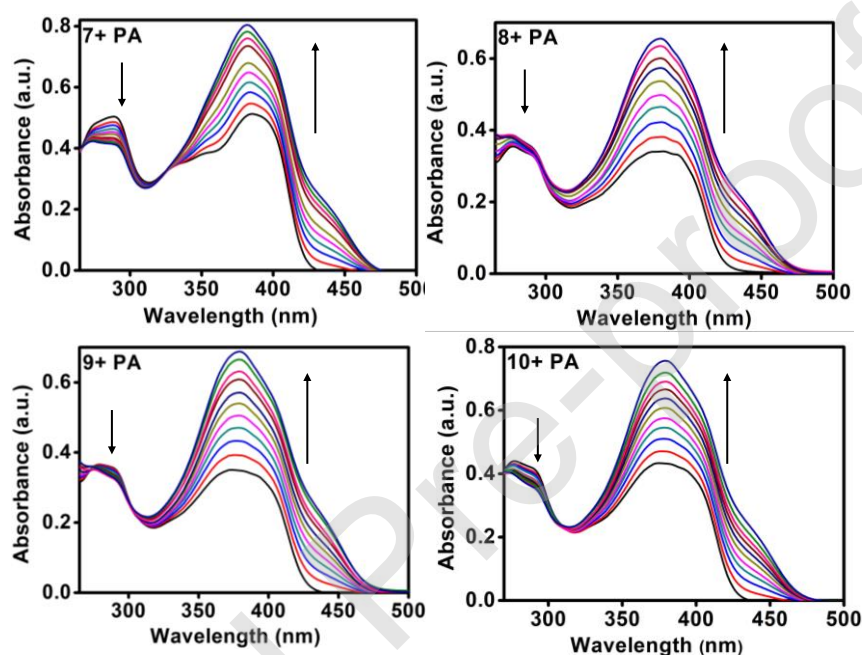


Figure 2. Interaction of PA with **7-10** (absorption spectra)

A constant volume of sensor molecule (10^{-5} M) was titrated against picric acid (10^{-4} M) and the changes in absorbance were recorded. Significant change was observed in both transitions. The spectra are depicted in the **Figure 2**. The absorption spectra confirms the interaction between the sensor molecule and PA, as there is no indication of PA's absorption peak (345 nm) [36]. The absorption spectra of the compounds tails at around 420 nm and the emission starts at 410 nm and this overlap enables the possibility of FRET energy transfer [37-41]. Electron rich methoxyphenyl and

thiophene groups in the molecules **9** and **10** have exhibited bathochromic shift of 6 and 4 nm, respectively during PA titration.

Table 2. Thermal properties and computational analysis of compounds **7-10**

C. No.	T _d (°C)	Computational (DFT) (eV)		
		HOMO	LUMO	Band gap
7	533	-5.18	-1.70	3.48
8	374	-5.16	-1.71	3.45
9	447	-5.10	-1.69	3.41
10	479	-5.18	-1.73	3.45

The absorbance is slowly increased and the band at 375 nm is red-shifted upon the addition of PA [42]. Remarkably, one new band appeared in the range of 420 to 480 nm (Figure 2). This new band increased the probability of overlap of the absorption with the emission spectra and opens the door for FRET mechanism [32]. Change in the absorption spectra revealed the complex formation/ interaction of picric acid with probe molecule. The compounds **7-10** show emission maxima at the range of 450-460 nm when excited at their corresponding absorption maxima. Upon the addition of PA to the sample solution, fluorescence intensity gradually decreased (**Figure 3**). On further addition of PA, fluorescence quenching was observed with a slight color change [43]. The compound **9** shows more quenching effect towards PA addition due to methoxyphenyl substitution. Pandith *et al.* reported anthracene carboxamide fluorescent probe with good response to picric acid over other NACs [44]. **Table 2** gives the HOMO-LUMO levels and decomposition temperature.

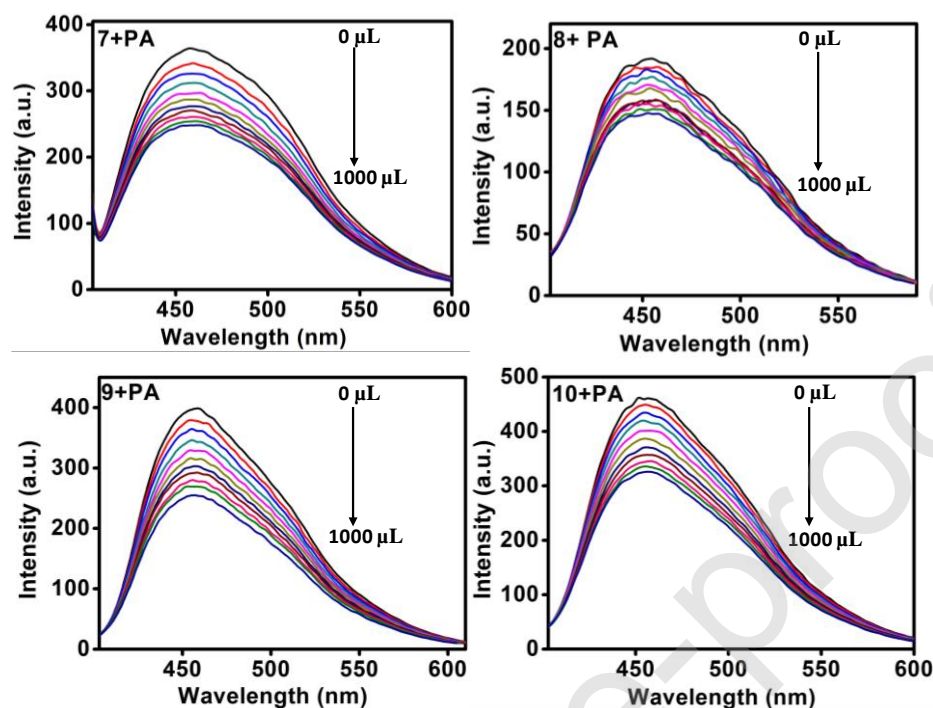


Figure3. Emission spectra of compounds **7-10** with picric acid, excited at 385, 381, 279, and 277 nm respectively

3.2 Stern-Volmer plot

Kinetics of sensing mechanism is explained with Stern-Volmer plot. Linearity of the plot explains the mechanism of quenching either static or dynamic [45]. The linear plots obtained for all the four sensing compounds clearly indicated the significance of $[Q]^1$ dependence in the interaction (**Figure 4**). The slope of Stern-Volmer plot indicates that the compound **9** exhibited better interactions with PA and the binding constant obtained as $1.46 \times 10^5 \text{ M}^{-1}$. This can be substantiated by the presence of electron rich methoxy group on TAA side arm, which can improve the interaction with electron deficient picric acid. The compounds **7** and **10** ($-H$ and thienyl substitution) shows $1.17 \times 10^5 \text{ M}^{-1}$ as the binding constant. Only slight variation in the binding constants is observed among the four compounds. The binding constant value of these new TAA functionalized phenanthrolines are ameliorated from the recent

reports. [43, 46] The detection limit was calculated to be at micro molar level for all the four compounds which is comparable with the similar type of sensor molecules [47-49].

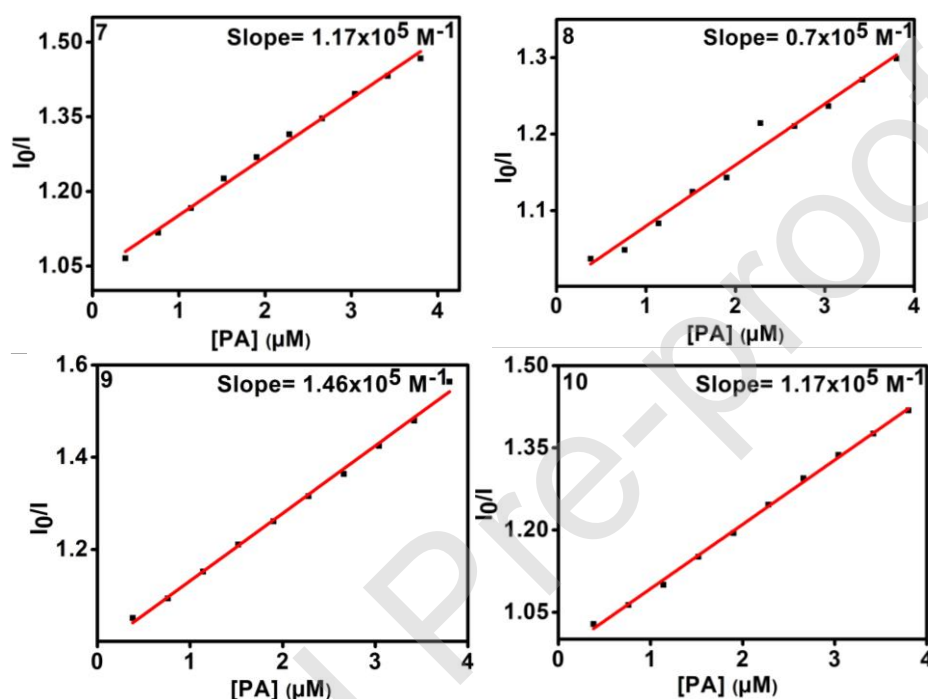


Figure 4. Stern-Volmer plot

3.3 Analyte selectivity studies

It is always important to address the selectivity of sensor molecule. In the present investigation, the selectivity was analyzed among other NACs such as 4-nitrobenzoic acid, 4-nitrophenol, 4-nitrobenzaldehyde and, 4-nitrotoluene. The interaction of the above mentioned nitro aromatic compounds with TAA functionalized phenanthrolines was scrutinized using UV-vis absorption spectroscopy technique. The responses in absorption spectra are given in the **Figure 5**. For the selectivity study, all the NACs

were taken in 10^{-4} M concentration. The absorption spectra were recorded before and after adding the NACs at fixed concentration of compounds. Among the NACs, picric acid shows significant change in the absorption intensity of the sensor molecules, whereas the other NACs have shown negligible effect. This observation is same for all the four compounds (compounds **7-10**). Although, the interaction of the four compounds with picric acid is appreciable than the others NACs, the difference in the absorption intensity is small. However, the formation of new band at around 430 nm (**Figure 2**) explains the better interaction with picric acid and no such band is observed with other NACs. Thus, we restricted the emission study for selectivity only to picric acid.

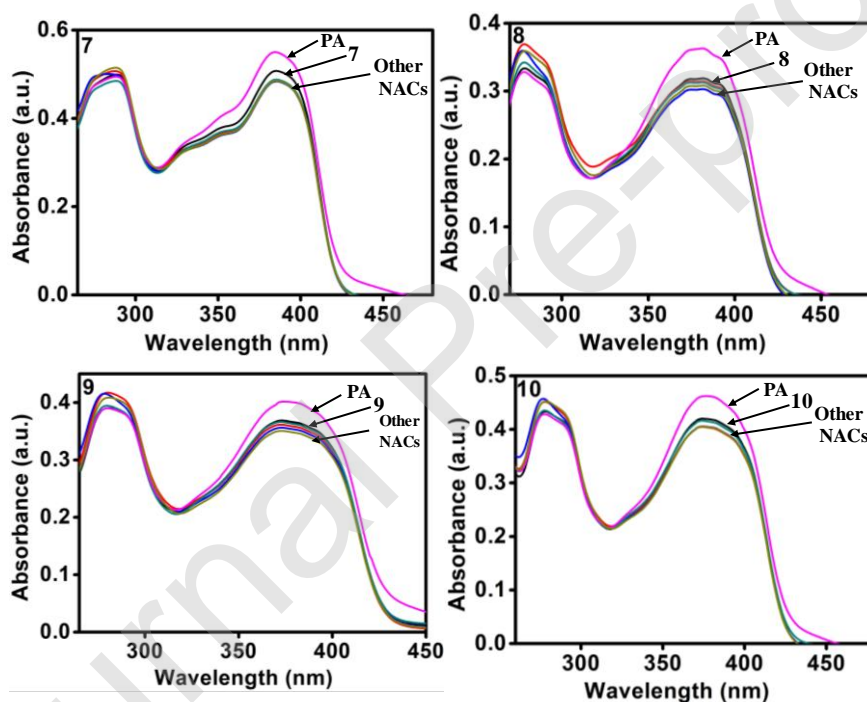


Figure 5. Interaction of sensors with PA and other NACs

3.4 Thermal properties

Thermal behaviour of the compounds (**7-10**) was analyzed by thermogravimetric analysis (TGA). All the compounds exhibited high thermal stability with a single decomposition in the region of 370-530 °C for 10 % by weight loss. Stepwise decomposition is not observed and thus the molecules are stable up to 530 °C. Tagare et al., [50] reported TAAs substituted with phenanthromidazoles in three arms for OLED application with a decomposition temperature of 450 °C. Hong and co-workers [51] reported on carbazole-imidazo [4,5-*f*]-1,10- phenanthroline hybrids for blue LED application. Those molecules had higher glass transition up to 240 °C but the decomposition point was less than 400°C. The TGA curves of the compounds **7-10** are shown in **Figure 6** and the extracted data are given in **Table 2**.

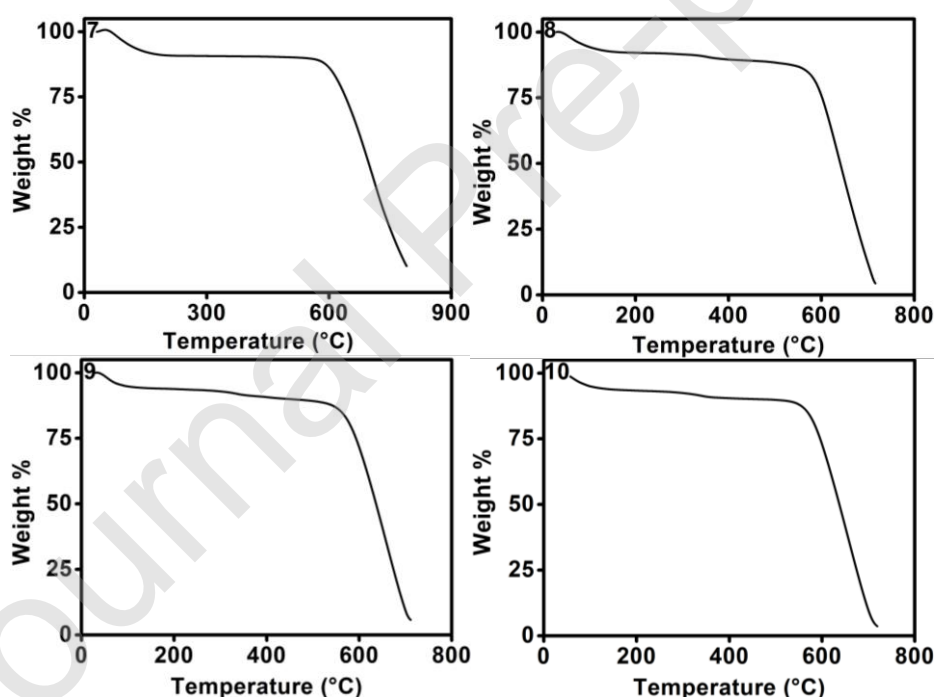


Figure6. TGA curves for the compounds **7-10**

3.5 Computational studies

The density functional theory (DFT) analysis was performed to get insight about the energy levels, energy distribution and the interaction between the sensor molecules and PA. The Frontier molecular orbital energy levels (HOMO and LUMO) were extracted using GaussView software and represented in the **Figures 7**. Frontier molecular energy values of PA (or picric acid) and sensor molecules ensure the feasible charge transfer from sensor molecules to picric acid. Energy transfer is feasible from the sensor molecules to PA with respect to their HOMO and LUMO levels. LUMO of picric acid (4.5eV) situated near the HOMO of sensor molecules (5.1eV) which can provide the possible way for energy transfer.

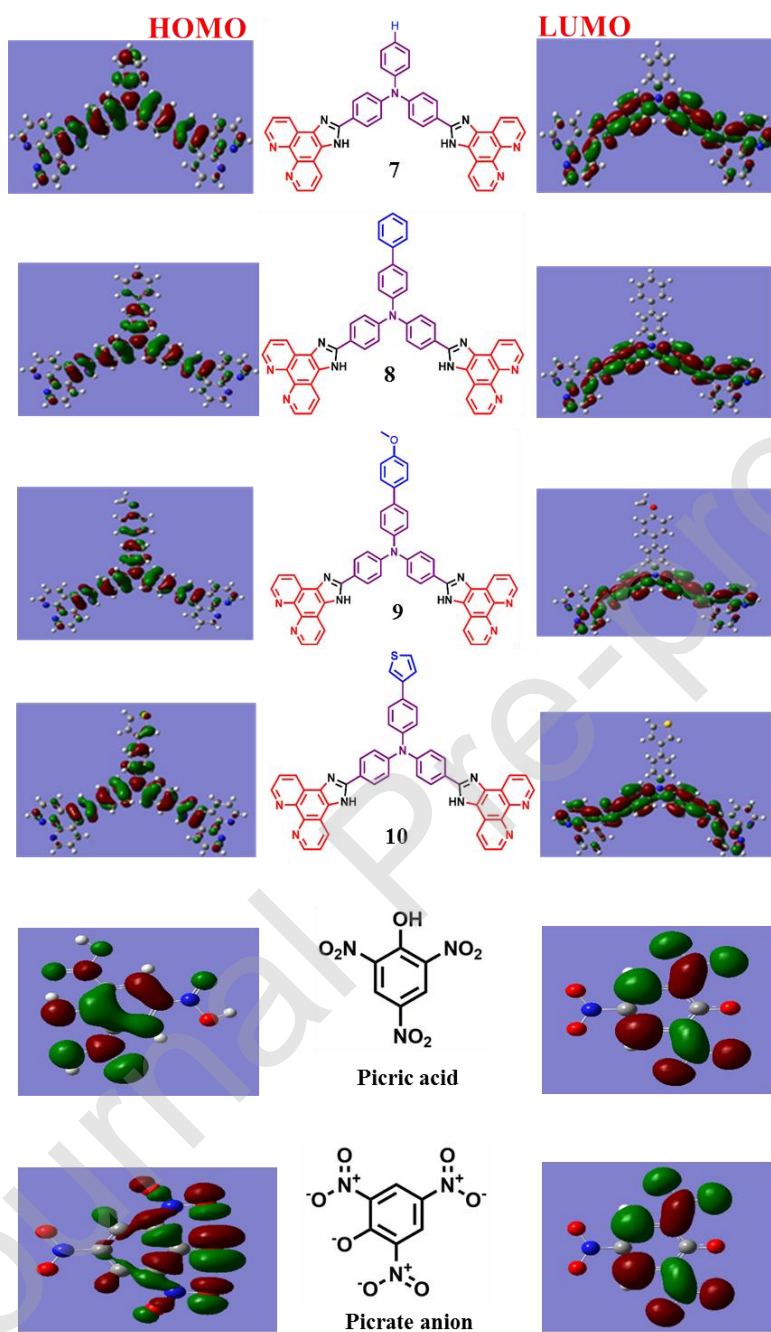


Figure 7. Qualitative representation of FMOs of molecules **7-10**, picric acid and picrate

4. Conclusion

Four new imidazo[4,5-*f*]-1,10-phenanthroline-triarylamines were designed for nitro compounds sensing. The compounds were successfully synthesized via microwave assisted synthesis with good yield and purity and well characterized using FT-IR, ESI-MS, ^1H and ^{13}C NMR. From the photophysical studies it was established that among different nitroaromatic compounds picric acid exhibited significant interaction. Among the molecules synthesized methoxy substituted compound shows high binding constant. Remarkably, one new band appeared in the range of 420 to 480 nm. This new band increased the probability of overlap of the absorption with the emission spectra and opens the door for FRET transfer mechanism. The detection limit was calculated to be at micro molar level for all the four compounds. These molecules can act as efficient fluorescence sensor for selective picric acid detection.

Conflicts of Interest Statement

The authors whose names are listed immediately below certify that they have NO affiliations with or involvement in any organization or entity with any financial interest (such as honoraria; educational grants; participation in speakers' bureaus; membership, employment, consultancies, stock ownership, or other equity interest; and expert testimony or patent-licensing arrangements), or non-financial interest (such as personal or professional relationships, affiliations, knowledge or beliefs) in the subject matter or materials discussed in this manuscript. Author names: The authors whose names are listed immediately below report the following details of affiliation.

References

- [1] J. Yang, T.M. Swager., Fluorescent porous polymer films as TNT chemosensors : electronic and structural effects, *J. Am. Chem. Soc.* (1998) 11864–11873, <https://doi.org/10.1021/ja982293q>.
- [2] F. Abbasi, A. Akbarinejad, N. Alizadeh., CdS QDs/N-Methylpolypyrrole Hybrids as Fluorescent Probe for Ultrasensitive and Selective Detection of Picric Acid. *Spectrochim. Acta - Part A Mol. Biomol. Spectrosc.* 216 (2019) 230–235, <https://doi.org/10.1016/j.saa.2019.03.032>.
- [3] D. T. Burton, K. R. Cooper, W. L. Goodfellow, D. H. Rosenblatt., Acute toxicity of picric acid and picramic acid to rainbow trout, *salmo gairdneri*, and american oyster, *crassostrea virginica*, *J. Am. Water Resour. Assoc.* 19 (1983) 641–648, <https://doi.org/10.1111/j.1752-1688.1983.tb02782.x>.
- [4] B. Niehus, W. Engewald., Identification and quantification of polar nitroaromatic compounds in explosive-contaminated waters by means of HPLC-ESI-MS-MS and HPLC-UV, *Chromatographia* 63 (2006) 1–11, <https://doi.org/10.1365/s10337-005-0703-8>.
- [5] E. P. Diamandis, T. P. Hadjiioannou., Catalytic determination of selenium with a picrate-selective electrode, *Analytica Chimica Acta* 123 (1981) 143–150, [https://doi.org/10.1016/S0003-2670\(01\)83167-6](https://doi.org/10.1016/S0003-2670(01)83167-6).
- [6] S. G. Metcalf, A. A. Okemgbo., A novel picric acid film sensor via combination of the surface enrichment effect of chitosan films and the aggregation- induced emission effect of siloles, *Abstr. Pap. Am. Chem. Soc* 218 (1999) 124, <https://doi.org/10.1039/B906946A>.
- [7] T. Gunnlaugsson, E. U. Akkaya, J. Yoon, T. D. James., Fluorescent chemosensors: the past, present and future, *Chem. Society Rev.* 46 (2017) 7105–7013, <https://doi.org/10.1039/C7CS00240H>.
- [8] S. Shanmugaraju, P. S. Mukherjee., Pi-Electron rich small molecule sensors for the recognition of nitroaromatics, *Chemcomm.* 51 (2015) 16014–16032, <https://doi.org/10.1039/C5CC07513K>.

- [9] P.P. Soufeena, T.A. Nibila, K.K. Aravindakshan., Coumarin Based Yellow Emissive AIEE Active Probe: A Colorimetric Sensor for Cu²⁺ and Fluorescent Sensor for Picric Acid, *Spectrochim. Acta - Part A Mol. Biomol. Spectrosc.* 223 (2019) 117201, <https://doi.org/10.1016/j.saa.2019.117201>.
- [10] B. Pramanik, N. Singha, D. Das., Sol-, Gel-, and Paper-based detection of picric acid at femtogram level by a short peptide gelator, *ACS Appl. Polym. Mater.* 1 (2019) 833–843, <https://doi.org/10.1021/acsapm.9b00071>.
- [11] S. Kumar, R. Kishan, P. Kumar, S. Pachisia, R. Gupta., Size-selective detection of picric acid by fluorescent palladium macrocycles, *Inorg. Chem.* 57 (2018) 1693–1697, <https://doi.org/10.1021/acs.inorgchem.7b02813>.
- [12] L. R. Adil, P. Gopikrishna, P. K. Iyer., Receptor-free detection of picric acid: A structural approach for designing aggregation-induced emission probes, *ACS Appl. Mater. Interfaces* 10 (2018) 27260–27268, <https://doi.org/10.1021/acsami.8b07019>.
- [13] H. Dong, W. Gao, F. Yan, H. Ji, H. Ju., Fluorescence resonance energy transfer between quantum dots and graphene oxide for sensing biomolecules, *Anal. Chem.* 82 (2010) 5511–5517, <https://doi.org/10.1021/ac100852z>.
- [14] T. Kowalczyk, Z. Lin, T. V. Voorhis., Fluorescence quenching by photoinduced electron transfer in the Zn²⁺ sensor zinpyr-1 : A computational investigation, *J. Phys. Chem. A* 114 (2010) 10427–10434, <https://doi.org/10.1021/jp103153a>.
- [15] T. M. Swager, The molecular wire approach to sensory signal amplification, *Acc. Chem. Res.* 31 (1998) 201–207, <https://doi.org/10.1021/ar9600502>.
- [16] V. Bhalla, A. Gupta, M. Kumar, D. S. S. Rao, S. K. Prasad., Self-assembled pentacenequinone derivative for trace detection of picric acid, *ACS Appl. Mater. Interfaces* 5 (2013) 672–679, <https://doi.org/10.1021/am302132h>.
- [17] M. Hussain, A. Nafady, T. Sherazi, R. Shah, A. Alsalmeh, M. S. Kalhor, S. A. Mahesar, S. Siddiqui., Cefuroxime derived copper nanoparticles and their application as colorimetric sensor for trace level detection of picric acid, *RSC Adv.* 6 (2016) 82882–82889, <https://doi.org/10.1039/C6RA08571G>.

- [18] R. Dheepika, R. Abhijnakrishna, P.M. Imran, S. Nagarajan., High performance p-channel and ambipolar OFETs based on imidazo [4, 5-f]-1, 10-phenanthroline-triarylamines RSC Adv 10, 22 (2020) 13043 <https://doi.org/10.1039/D0RA00210K>.
- [19] R. Dheepika, P.M. Imran, N.S.P Bhuvanesh, S. Nagarajan., Solution-processable unsymmetrical triarylamines: Towards high mobility and ON/OFF ratio in bottom-gated OFET, Chem. Eur. J. 25 (2019) 15155, <https://doi.org/10.1002/chem.201903450>.
- [20] P. Devibala, R. Dheepika, P. Vadivelu, S. Nagarajan., Synthesis of aroylbenzoate-based push-pull molecules for OFET Applications, ChemistrySelect 4 (2019) 2339, <https://doi.org/10.1002/slct.201803394>.
- [21] R. Chennoufi, H. Bougherara, N. Gagey-eilstein, B. Dumat, E. Henry, F. Subra, S. Bury-moné, F. Mahuteau-betzer, P. Tauc, E. Deprez., Mitochondria-targeted triphenylamine derivatives activatable by two-photon excitation for triggering and imaging cell apoptosis, Nat. Publ. Gr. (2016) 1–12, <https://doi.org/10.1038/srep21458>.
- [22] R. Dheepika, R. A. Shaji, P.M. Imran, S. Nagarajan., Improving device performance of p-type organic field-effect transistor using butterfly like triarylamines Organic electronics (2019) 105568 <https://doi.org/10.1016/j.orgel.2019.105568>
- [23] P.P. Kumavata, P.K. Baviskarb, B. R. Sankapal, D. S. Dalal., Facile synthesis of D- π -A structured dyes and their applications towards cost effective fabrication of solar cell as well as sensing of hazardous Hg (II), RSC Adv. 6 (2016) 106453–106464, <https://doi.org/10.1039/C6RA18712A>.
- [24] A.K. Mahapatra, G. Hazra, N.K. Das, S. Goswami., A q highly selective triphenylamine-based indolylmethane derivatives as colorimetric and turn-off fluorimetric sensor toward Cu²⁺ detection by deprotonation of secondary amines, Sensors and Actuators B: Chemical. 156 (2011) 456–462, <https://doi.org/10.1021/acsomega.9b00970>.

- [25] J. B. Arockiam, S. Ayyanar., Benzothiazole, Pyridine Functionalized Triphenylamine Based Fluorophore for Solid State Fluorescence Switching, Fe³⁺ and Picric Acid Sensing. *Sensors Actuators B. Chem.* 242 (2016) 535–544. <https://doi.org/10.1016/j.snb.2016.11.086>.
- [26] E. V. Verbitskiy, Y. A. Kvashnin, A. A. Baranova, K.O. Khokhlov, R. D. Chuvashov, E. Schapov, Y. A. Yakovleva, E. F. Zhilina, A. V. Shchepochkin, N. I. Makarova, E. V. Vetrova, A. V. Metelitsa, G. L. Rusinov, O. N. Chupakhin, V. N. Charushin., Synthesis and Characterization of Linear 1, 4-Diazine-Triphenylamine – Based Selective Chemosensors for Recognition of Nitroaromatic Compounds and Aliphatic Amines, *Dye. Pigment.* 178 (2020) 1–10. <https://doi.org/s://doi.org/10.1016/j.dyepig.2020.108344>.
- [27] G. Sathiyam, B. Balasubramaniam, S. Ranjan, S. Chatterjee, P. Sen, A. Garg., A Novel Star-Shaped Triazine-Triphenylamine e Based Fluorescent Chemosensor for the Selective Detection of Picric Acid, *Mater. Today Chem.* 12 (2019) 178–186. <https://doi.org/10.1016/j.mtchem.2019.01.002>.
- [28] X. Q. Yao, G. B. Xiao, H. Xie, D. D. Qin, H. C. Ma, J. C. Liu, P. J. Yan., Two Triphenylamine-Based Luminescent Metal-Organic Frameworks as a Dual-Functional Sensor for the Detection of Nitroaromatic Compounds and Ofloxacin Antibiotic, *CrystEngComm.* 21 (2019) 2559–2570. <https://doi.org/10.1039/C8CE02122H>.
- [29] K. Duraimurugan, R. Balasaravanan, A. Siva., Electron Rich Triphenylamine Derivatives (D- π -D) for Selective Sensing of Picric Acid in Aqueous Media, *Sensors Actuators, B Chem.* 231 (2016) 302–312. <https://doi.org/10.1016/j.snb.2016.03.035>.
- [30] Wu, H.; Tao, F.; Cui, Y.; Guo, L. Two Triphenylamine-Based AIE Materials for the Detection of PA in Aqueous Medium. *Mater. Chem. Phys.* **2020**, *240* (July 2019), 122141. <https://doi.org/10.1016/j.matchemphys.2019.122141>.
- [31] P.B. Pati, S.S. Zade., Highly emissive triphenylamine based fluorophores for detection of picric acid, *Tetrahedron Lett.* 55 (2014) 5290–5293.

- [32] A. Chowdhury, P.S. Mukherjee., Electron-rich triphenylamine-based sensors for picric acid detection, JOC Artic. 80 (2015) 4064–4075, <https://doi.org/10.1021/acs.joc.5b00348>.
- [33] M. Muralisankar, R. Dheepika, J. Haribabu, C. Balachandran, S. Aoki, N.S.P. Bhuvanesh, S. Nagarajan., Design, Synthesis, DNA/HSA binding, and cytotoxic activity of halfsandwich Ru(II)-arene complexes containing triarylamine-thiosemicarbazone hybrids, ACS Omega, 4 (2019) 11712, <https://doi.org/10.1021/acsomega.9b01022>.
- [34] X. Zhang, H. Yu, Y. Xiao., Replacing phenyl ring with thiophene: an approach to longer wavelength aza-dipyrrromethene boron difluoride (Aza-BODIPY) dyes, J. Org. Chem. 77 (2012) 669–673, <https://doi.org/10.1021/jo201413b>.
- [35] R. Dheepika, S. Sonalin, P.M. Imran, S. Nagarajan., Unsymmetrical starburst triarylamine: synthesis, properties, and characteristics of OFETs, J. Mater. Chem. C 6 (2018) 6916–6919, <https://doi.org/10.1039/C8TC02017E>.
- [36] Y. Wu, S. Luo, L. Cao, K. Jiang, L. Wang, J. Xie, Z. Wang., Self-assembled structures of N-alkylated bisbenzimidazolyl naphthalene in aqueous media for highly sensitive detection of picric acid, Analytica Chimica Acta. 976 (2017), 74–83, <https://doi.org/10.1016/j.aca.2017.04.022>.
- [37] H. Fu, L. Yan, N. Wu, L. Ma, S. Zang., Dual-Emission MOF I Dye Sensor for Ratiometric Fluorescence Recognition of RDX and Detection Of a broad class of nitro-compounds, J. Mater. Chem. A Mater. energy Sustain. 6 (2018) 9183–9191. <https://doi.org/10.1039/C8TA02857E>.
- [38] D. Dinda, A. Gupta, B. K. Shaw, S. Sadhu, S. K. Saha., Highly Selective Detection of Trinitrophenol by Luminescent Functionalized Reduced Graphene Oxide through FRET Mechanism, Appl. Mater. Interfaces 6 (2014) 10722–10728. <https://doi.org/10.1021/am5025676>.
- [39] M. Kumar, V. Kumar, A. Javed, S. Satapathi., Nano-Structures & Nano-Objects Graphene Quantum Dots and Carbon Nano Dots for the FRET Based Detection of Heavy Metal Ions, Nano-Structures & Nano-Objects 19 (2019) 100347. <https://doi.org/10.1016/j.nanoso.2019.100347>.

- [40] V. Kumar, N. Choudhury, A. Kumar, P. De, S. Satapathi., Poly-Tryptophan / Carbazole Based FRET-System for Sensitive Detection of Nitroaromatic Explosives, *Opt. Mater. (Amst)*. 100 (2020) 109710. <https://doi.org/10.1016/j.optmat.2020.109710>.
- [41] V. V. Koppal, P. G. Patil, R. M. Melavanki, R. A. Kusanur, U. Onumashi, N. R. Patil., Exploring the influence of Silver Nanoparticles on the Mechanism of Fluorescence Quenching of Coumarin Dye Using FRET, *J. Mol. Liq.* 292 (2019) 111419. <https://doi.org/10.1016/j.molliq.2019.111419>.
- [42] S. Kumari, S. Joshi, T.C. Cordova-sintjago, D.D. Pant, R. Sakhuja., Highly sensitive fluorescent imidazolium-based sensors for nanomolar detection of explosive picric acid in aqueous medium, *Sensors Actuators B. Chem.* 229 (2016) 599–608, <https://doi.org/10.1016/j.snb.2016.02.019>.
- [43] B. Roy, A. K. Bar, B. Gole, P.S. Mukherjee., Fluorescent tris-imidazolium sensors for picric acid explosive, *J. Org. Chem.* 78 (2013) 1306–1310, <https://doi.org/10.1021/jo302585a>.
- [44] A. Pandith, A. Kumar, J. Lee, H. Kim., 9-Anthracenecarboxamide fluorescent probes for selective discrimination of picric acid from mono- and di-nitrophenols in ethanol, *Tetrahedron Lett.* 56 (2015) 7094–7099, <https://doi.org/10.1016/j.tetlet.2015.11.017>.
- [45] J. R. Lakowicz., *Principles of fluorescence spectroscopy*, Third edit.; (2016)
- [46] K. Jiang, S. Luo, C. Pang, B. Wang, H. Wu, Z. Wang., A functionalized fluorochrome based on quinoline-benzimidazole conjugate : from facile design to highly sensitive and selective sensing for picric acid, *Dyes and Pigments* 162 (2019) 367–376, <https://doi.org/10.1016/j.dyepig.2018.10.041>.
- [47] S. Chaudhary, H. Sharma, M. D. Milton., Novel 2-Arylbenzothiazoles: Selective Chromogenic and Fluorescent Probes for the Detection of Picric Acid, *ChemistrySelect* 3 (2018) 4598–4608. <https://doi.org/10.1002/slct.201800645>.
- [48] S. Nath, S. K. Pathak, B. Pradhan, R. K. Gupta, K. A. Reddy, G. Krishnamoorthy, A. S. Achalkumar., A Sensitive and Selective Sensor for Picric

- Acid Detection with a Fluorescence Switching Response, *New J. Chem.* 42 (2018) 5382–5394. <https://doi.org/10.1039/c7nj05136k>.
- [49] J. Sahoo, D. S. Lakshmi, E. Suresh, P. S. Subramanian., Selective and Sensitive Detection of Picric Acid in Aqueous, Sol-Gel and Solid Support Media by Ln(III) Probes, *Sensors Actuators, B Chem.* 250 (2017) 215–223. <https://doi.org/10.1016/j.snb.2017.04.170>.
- [50] J. Tagare, H. Ulla, B. Kajjam, M.N. Satyanarayan., Star-Shaped Phenanthroimidazole-Triphenylamine-Based Yellow Organic Emitter for Organic Light Emitting Diodes. *Chem. Sel.* 2 (2017) 2611–2620, <https://doi.org/10.1002/slct.201700056>.
- [51] H. Huang, Y. Wang, S. Zhuang, X. Yang, L. Wang, C. Yang, Simple Phenanthroimidazole/Carbazole Hybrid Bipolar Host Materials for Highly Efficient Green and Yellow Phosphorescent Organic Light-Emitting Diodes, *J. Org. Chem.* 116 (2012) 19458–19466, <https://doi.org/10.1021/jp305764b>.